

## Poly(DMAEMA-co-MPS) 코팅 메조포러스 실리카 나노입자 약물전달체 제조 및 pH 감응형 on-off 방출 특성분석

Mohammad Hegazy<sup>\*,\*\*,\*†</sup>, Nahla Rahoui<sup>\*\*\*\*</sup>, Ahmed Abou- Elyazed<sup>\*\*\*</sup>, Diao Eldin Fouad<sup>\*\*\*\*\*</sup>,  
Xin Huang<sup>\*,\*†</sup>, and Yudong Huang<sup>\*,\*†</sup>

\*MIIT Key Laboratory of Critical Materials Technology for New Energy Conversion and Storage, Key Laboratory of Microsystems and Microstructures Manufacturing, Ministry of Education, School of Chemistry and Chemical Engineering, Harbin Institute of Technology

\*\*Department of Chemistry, Faculty of Science, Menoufia University

\*\*\*College of Material Science and Chemical Engineering, Harbin Engineering University

\*\*\*\*Forensic authority, Ministry of Justice

\*\*\*\*\*Research and Development Institute in Industry and Defense Technologies

(2019년 1월 14일 접수, 2019년 2월 27일 수정, 2019년 3월 2일 채택)

## Poly(DMAEMA-co-MPS) Coated Mesoporous Silica Nanoparticles as Smart Drug Carriers with pH-controlled on-off Release

Mohammad Hegazy<sup>\*,\*\*,\*†</sup>, Nahla Rahoui<sup>\*\*\*\*</sup>, Ahmed Abou- Elyazed<sup>\*\*\*</sup>, Diao Eldin Fouad<sup>\*\*\*\*\*</sup>,  
Xin Huang<sup>\*,\*†</sup>, and Yudong Huang<sup>\*,\*†</sup>

\*MIIT Key Laboratory of Critical Materials Technology for New Energy Conversion and Storage, Key Laboratory of Microsystems and Microstructures Manufacturing, Ministry of Education, School of Chemistry and Chemical Engineering, Harbin Institute of Technology, Harbin 150001, China

\*\*Department of Chemistry, Faculty of Science, Menoufia University, Shebin El-Kom 32511, Egypt

\*\*\*College of Material Science and Chemical Engineering, Harbin Engineering University, Harbin 150001, China

\*\*\*\*Forensic authority, Ministry of Justice, Egypt to Forensic Authority, Ministry of Justice, Cairo, Egypt

\*\*\*\*\*Research and Development Institute in Industry and Defense Technologies, Blida, BP. 09000, Algeria

(Received January 14, 2019; Revised February 27, 2019; Accepted March 2, 2019)

**Abstract:** In this paper, pH-responsive nanocarriers based on mesoporous silica nanoparticles (MSN) modified with the pH-sensitive polymer: poly(*N,N*-dimethylaminoethyl methacrylate) (PDMAEMA) were constructed, characterized and tested to evaluate their efficacy as drug delivery systems (DDS). The hybrid nanocarriers were synthesized successfully via a simultaneous copolymerization reaction between two monomers; 2-dimethylamino-ethylmethacrylate (DMAEMA) and 3-methacryloxypropyltrimethoxysilane (MPS) within the mesopores of MSN. Exploiting the polymerizable moiety of MPS together with its alkoxy silane moiety susceptible to condensation with silanols surface onto silica, MPS comonomer can act as a bridge for yielding a robust and simple hybrid consisting of MSN-P(DMAEMA-co-MPS). In addition, the grafted PDMAEMA serves as efficient gatekeeper to adjust the encapsulation and *in vitro* release of cargos loaded inside the pores by altering pH values of the medium. These hybrid nanoparticles showed a high loading capacity with quick release in acidic pH, which exists mainly in the diseases environments e.g. inflammatory and cancerous sites.

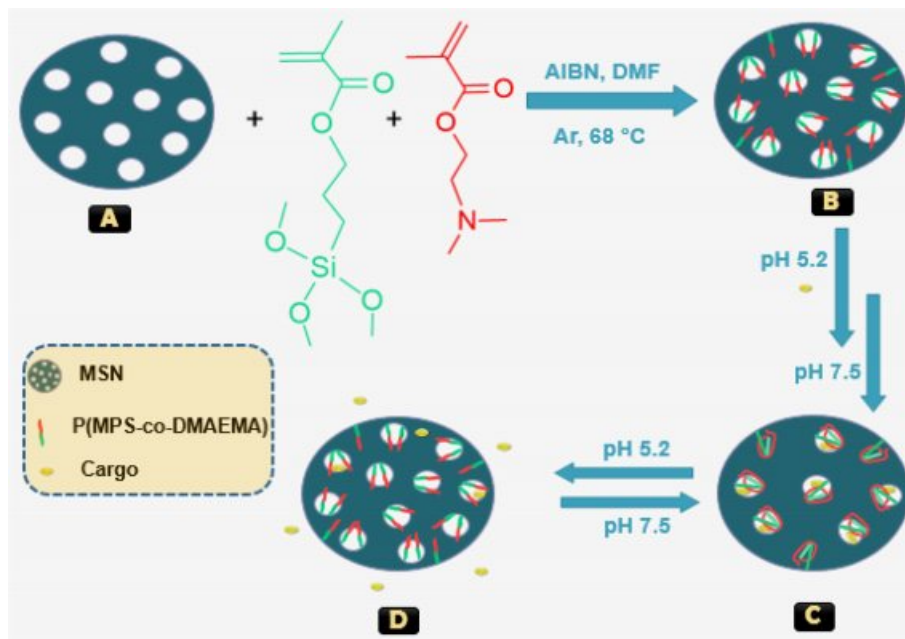
**Keywords:** pH-responsive release, mesoporous silica nanoparticles, poly(*N,N*-dimethylaminoethyl methacrylate), polymer coating, controlled drug delivery.

†To whom correspondence should be addressed.  
dr\_hegazy2000@yahoo.com, ORCID<sup>®</sup>0000-0002-9335-7687  
xinhuang@hit.edu.cn, ORCID<sup>®</sup>0000-0002-1858-2956  
huangyd@hit.edu.cn, ORCID<sup>®</sup>0000-0002-8019-6618  
©2019 The Polymer Society of Korea. All rights reserved.

## Introduction

Polymeric smart materials are very advantageous for lots of applications, such as, dental restorations, viable artificial cell walls, synthetic protocells, automotive exterior lamps, H<sub>2</sub> production, photocatalytic decomposition of organic dyes, wastewater treatment, ion absorbance capacity, energy operations, bone regeneration, cancer therapy, photothermal and photodynamic effects.<sup>1-11</sup> Recently, nanomaterials with size of 1-1000 nm are necessary for drug delivery research area, since the mentioned size is identical to that of a variety of biological macromolecules, e.g. siRNA, DNA and proteins,<sup>12</sup> leading to high-quality and developed therapeutic drug delivery systems (DDS). A promising example is MSN, which has been studied extensively for bioscience purposes e.g. cell tracing, hyperthermia treatment, cancer therapy, cellular uptake, diagnosis as well as MRI imaging, due to their nontoxicity, biocompatibility, facility of surface functionalization and controllable mesopore structures.<sup>13</sup> In addition, MSN could be used alone as stimuli-responsive drug/gene nanocontainers, or together with some other nanomaterials such as gold nanorods, silver nanoparticles, quantum dots or magnetic nanoparticles (with 4 basic structures including: core-shell structure, embedded structure, rattle-type particles and magnetite “Fe<sub>3</sub>O<sub>4</sub>” capped mSiO<sub>2</sub>) to further improve the corresponding properties and

applications.<sup>14,15</sup> Multiple strategies of smart polymer delivery systems such as chemical triggers,<sup>16</sup> thermally induced release,<sup>17</sup> redox responsive reactions<sup>18</sup> and magnetically initiated release<sup>19</sup> were also anchored onto the amorphous surface of silica particles to increase cargo loading along with modulating rate or period of cargo release processes. These polymers can work as smart caps or gatekeepers and thus organize the release of the encapsulated cargos inside the MSN pores. The pH responsive polymers are very useful in treating various diseases especially cancer tissues. It was found that, the pH of cancer cells are often lower (i.e. more acidic) than that of the neighboring normal cells because of the high rates of glycolysis process in tumor cells.<sup>20</sup> Hong *et al.* coated poly(acrylic acid) (PAA) onto the surface of MSN through RAFT polymerization technique, yielding a nanodevice consisting of a pH-responsive PAA nanoshell as a smart nanovalve and MSN as guest nanocarriers.<sup>21</sup> Recently, Zhang and co-workers studied the controlled release of cargos from mesoporous silica nanoparticles via the pH-sensitive poly(2-(diethylamino)-ethyl methacrylate) (PDEAEMA) via surface-initiated ATRP.<sup>22</sup> The methyl analogue: poly(*N,N*-dimethylaminoethyl methacrylate) (PDMAEMA) was demonstrated as a very hydrophobic or rarely water-soluble at both alkaline or neutral pH with uncharged collapsed chains, whereas it converts into a weak cationic polyelectrolyte in acidic solution with high solubil-



**Scheme 1.** Synthetic route of grafting P(DMAEMA-co-MPS) on MSN surface, followed by drug loading and release process. The steps including: bare MSN (A); P(DMAEMA-co-MPS)-coated MSN hybrid (B); DOX-loaded hybrid (C); DOX-released hybrid (D).

ities, protonated chains, and extended conformations.<sup>23</sup> In this context, we designed a facile approach to attach the pH-sensitive gatekeeper PDMAEMA with the silicon derivative polymer PMPS onto the surface of MSN using a simple one-step condensation and polymerization reaction. The obtained nano-system has been characterized via several methods to evidence a successful synthesis. The release behavior of doxorubicin (DOX) as an antitumor drug from this nanocontainer was investigated at three chosen pHs and the results demonstrated that the drug could be simply loaded into the interior pores of MSN, then followed by on-off controlled release behavior according to pH changes (Scheme 1). This work therefore explains a significant consideration for the suitable choice of MSN with functionalized polymers on them for the potential applications in the targeted synthesis of pH DDS.

## Experimental

**Materials and Reagents.** All chemicals expressed in the preparation processes including reagents and solvents were supplied by Sigma-Aldrich and they were with analytical grade of purity so used as received except DMAEMA and MPS monomers. The liquid monomers were purified by passing them through an alumina column for inhibitors removing, then exposed to vacuum distillation. The aqueous solutions were obtained through Milli-Q water.

**Characterization Methods.** UV-Visible absorption spectra with a scanning range from 200 to 900 nm were collected on Lambda 750S spectrophotometer (PerkinElmer, USA). Transmission electron microscopy (TEM) analysis was undertaken on a JEM21400, using a LaB6 filament. Samples were obtained by adding one droplet of nanoparticle solution (0.1 mg/mL) on a carbon film coating copper grid and the specimens were then dried in vacuum for one day. Zeta potential analysis and size distribution (via dynamic light scattering 'DLS') for sample solutions (0.2 mg/mL, pH 6.8, 5.0 mM PBS buffer) were carried out at 25 °C via a ZETASIZER Nano-series instrument (Malvern Instrument, United Kingdom). Fourier transform infrared (FTIR) analysis was obtained via Nicolet Nexus-440 FTIR spectrometer. The samples were mixed with solid KBr which used also as the background ( $\approx 3$  mg sample per 400 mg) and then spectra were scanned over a range of 450-4000  $\text{cm}^{-1}$ .

**Preparation of Experimental Materials.** Preparation of P(DMAEMA-co-MPS)-coated MSN Hybrid: First, MCM-41-like nanoparticles were prepared by the previously reported

literature.<sup>24</sup> Subsequently, 70 mg of the obtained materials were transferred into a three neck round bottom flask and dissolved via sonication in 5 mL ethanol solution containing 17.5 mg of DMAEMA, 1.38 mg of MPS and 0.6 mg of AIBN at 25 °C for 20 min. The polymerization flask was flushed with Ar before sealing and heating at  $70 \pm 1$  °C. After 18 h, the polymerization was stopped through exposing to air, then the hybrid was washed by pure water two times and obtained after freeze drying for 24 h.<sup>25,26</sup>

**Drug Loading Experiments<sup>27</sup>:** DOX as model drug was chosen for loading experiments. Briefly, the obtained hybrid and DOX were dispersed under overnight magnetic stirring in 10 mL of buffer solution (2 mM, pH 5.2) at room temperature in the dark. The DOX hybrid (DOX@hybrid) was collected by centrifugation at 8000 rpm for 15 min using ultra-pure water (pH 6.998) followed by washing two times with PBS buffer solution (pH 7.5) to eliminate any adsorbed Dox molecules at the surface of the hybrid (Scheme 1, step B-C). The DOX loading was detected by UV-visible spectra through monitoring the absorbance at 480 nm. A similar way was used for bare MSN to produce DOX@MSN. The drug loading content (DLC) was estimated according to eq. (1).

$$\text{DLC (\%)} = \frac{\text{weight of loaded DOX}}{\text{weight of DOX@hybrid or DOX@MSN}} \times 100 \quad (1)$$

**In Vitro Drug Release Experiments:** The *in vitro* drug release experiments for DOX@hybrid were performed in phosphate buffer saline (PBS) solution at pH 5.2, 6.4 and 7.5 (which is the storage pH of the used drug), respectively at 25 °C. The release behaviors were obtained by detecting the absorbance peak of DOX at 480 nm at given time periods. In general, all experiments were carried out three times and the average values were plotted. After drug loading processes, the release content (RC) was estimated according to eq. (2) as follows:

$$\text{RC (\%)} = \frac{\text{Conc. of released drug in medium}}{\text{Conc. of DOX in DOX@hybrid or DOX@MSN}} \times 100 \quad (2)$$

## Results and Discussion

**Synthesis and Characterization of P(DMAEMA-co-MPS)-coated MSN Hybrid.** First, MSN was prepared as a precursor for the hybrid formation. The morphological analysis of the prepared MSN, obtained via transmission electron microscope (TEM), indicates well spherical shaped nanopar-

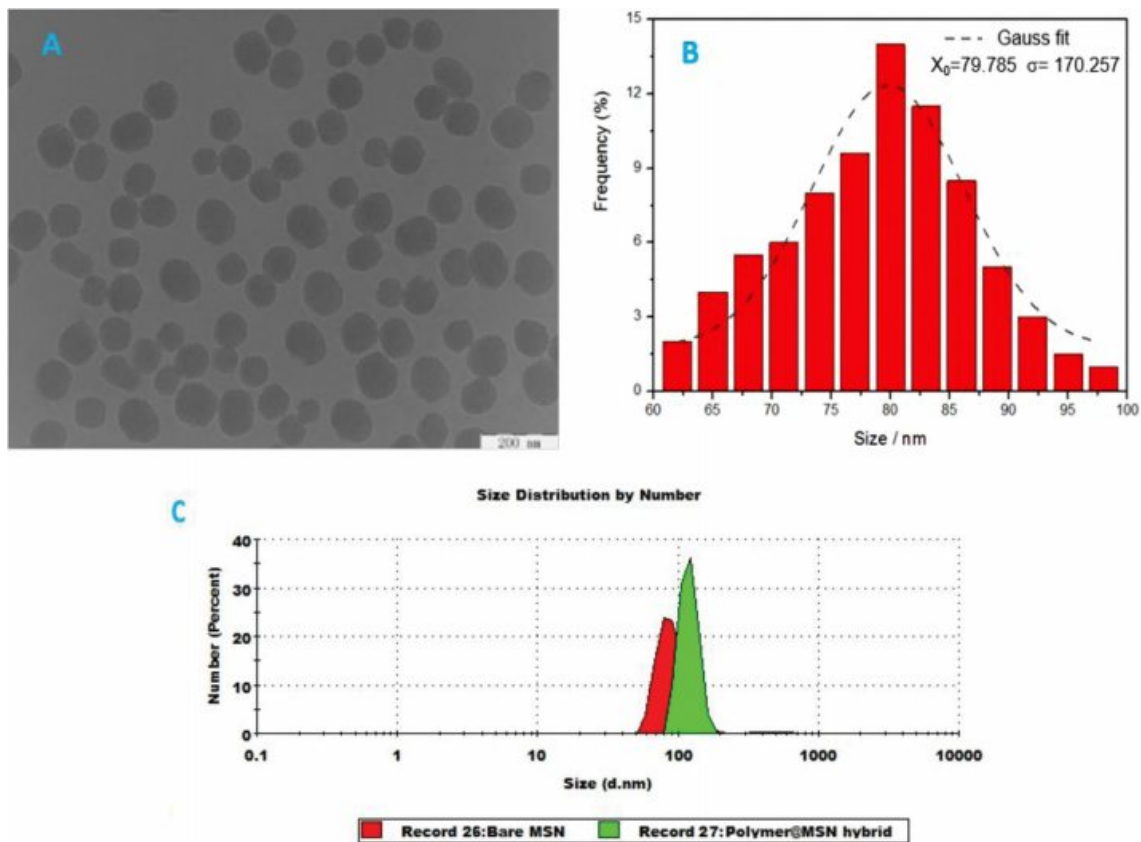


**Figure 1.** (A) TEM image of the prepared MSN with scale bare of 200 nm; (B) its corresponding particle size distribution plot (the median value and standard deviation were calculated by fitting Gaussian to the histogram); (C) size distributions of bare MSN (red) & polymer@MSN hybrid (green) in 5.0 mM PBS buffer solution (pH 6.8) determined by DLS, where hydrodynamic diameter were 78.8 nm and 122.4 nm, respectively.

ticles with uniform existence (Figure 1A). The average particle size was around ~80 nm according to size distribution measurements (Figure 1B). In addition, the average size of MSN was calculated by DLS and noticed to be about 78.8 nm, which was close to that obtained from TEM. Also, from the DLS analysis (Figure 1C), there was an observed increase in the hydrodynamic diameter from 78.8 to 122.4 nm after conjugating the copolymer layer onto the silica surface, which indicates a successful silica-coating with the polymeric shell.

The structural analysis and surface chemistry of either MSN before or after modification with the copolymer layer to form P(DMAEMA-*co*-MPS)-coated MSN hybrid, were confirmed by several techniques, such as FTIR analysis, UV-visible spectra and zeta potential ( $\zeta$ ) measurements. As revealed by FTIR spectra (Figure 2(a)), the existence of absorption bands at 1085 and 797  $\text{cm}^{-1}$  that related to stretching and bending vibrations of Si-O, respectively, was observed in all synthesized silica samples, whether before or after the modification

process, confirming the presence of silica framework.<sup>28</sup> More particular, MSN-CTAB had the typical aliphatic C-H stretching vibrations at 2925 and 2854  $\text{cm}^{-1}$  together with C-H bending vibration at 1469  $\text{cm}^{-1}$ . After CTAB removal in order to construct MSN, two characteristic O-H peaks derived from silanol groups (Si-OH) were generated at 3452 and 1630  $\text{cm}^{-1}$  for stretching and bending vibrations, respectively, with obvious reducing in C-H peak intensities, indicating a successful removing of that surfactant.<sup>29</sup> Compared with the FTIR spectrum of MSN, a new peak was detected at 1731  $\text{cm}^{-1}$  within the FTIR spectrum of the final hybrid, related to the stretching vibration of a newly formed ester group, while the C-H peaks were appeared again at 2923, 2853, and 1464  $\text{cm}^{-1}$ .<sup>30</sup> These results thence prove the successful anchoring of the copolymer on MSN. The corresponding chemical structures of MSN-CTAB, MSN and MSN-P (DMAEMA-*co*-MPS) were represented in Figure 2(b).

Furthermore and from Figure 3,  $\zeta$  decreases gradually by pH

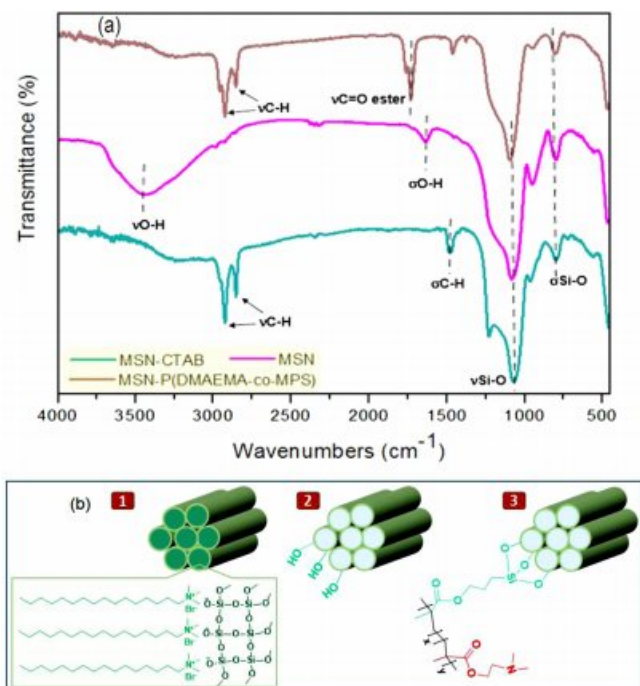


**Figure 2.** (a) FTIR spectra of MSN-CTAB, MSN and MSN-P(DMAEMA-co-MPS) nanoparticles; (b) chemical structures of MSN-CTAB '1', MSN '2' and MSN-P(DMAEMA-co-MPS) '3'.

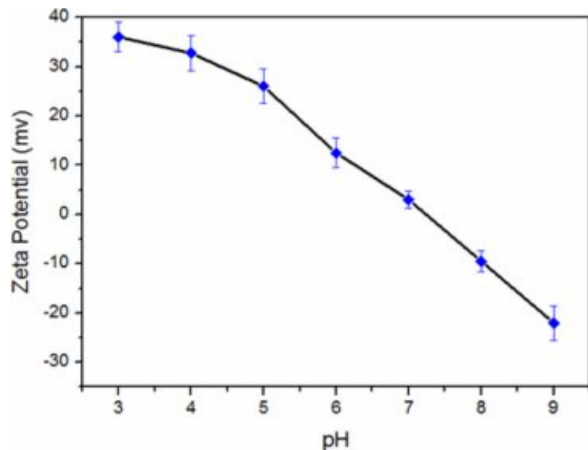


**Figure 3.** Zeta potential values obtained from pH-dependent particle experiments for as-synthesized polymer@MSN hybrid.

increasing. This could be attributed to the tertiary amine groups in PDMAEMA in which low pH media can acquire a proton and the polymer follows the coil soluble structure, whereas in high pH media it collapses into insoluble case because of the hydrophobic interaction between such polymeric chains. From the  $\zeta$  (pH) function, the critical pH of PDMAEMA to close the mesopores was found to be around pH 7.21 which is still less than human blood environment (pH

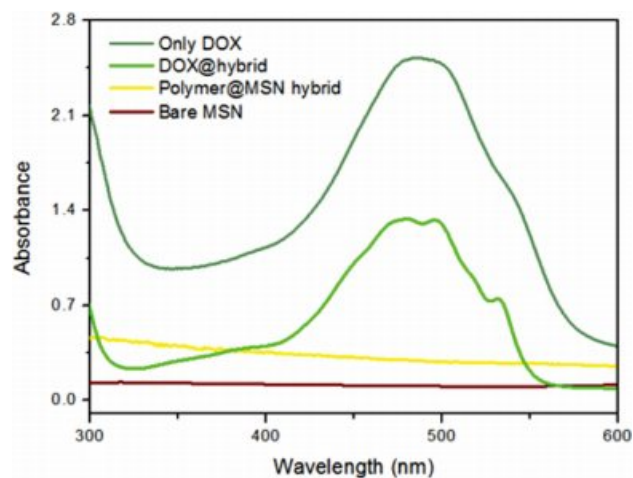


**Figure 4.** The normalized UV-vis spectra for bare MSN, polymer@MSN hybrid, DOX@hybrid and free DOX.

7.4). This means that in case of the system will be used as a smart drug delivery container, the release of hybrid encapsulated DOX can be triggered only when reaching the pathological sites where the pH is weakly acidic (Scheme 1, steps B–D).

In addition, Figure 4 demonstrates that no UV absorbance for whether bare MSN or its corresponding hybrid containing the copolymer layer as there is no observed conjugation within these moieties, which reflects the successful synthesis.<sup>31–33</sup> By contrast, when the hybrid thereafter incorporated with DOX to yield DOX@hybrid, it gives a significant new peak at 480 nm which is still lower intensity than the pure DOX peak, indicating a successful encapsulation process of this drug within MSN pores.

**pH Controlled Loading & Release Results.** First, different concentrations ranging from 0.0005 to 0.1 mg.mL<sup>-1</sup> of DOX were measured via UV-Vis spectrophotometer at 480 nm (Figure 5(a)), then the corresponding linear calibration curve for such concentrations was obtained consistently (with a pretty good R<sup>2</sup> value) for the detection of DOX amounts loaded in both DOX@MSN or DOX@hybrid as shown in Figure 5(b). The drug loading content (DLC) for DOX@hybrid was 18.6 ± 0.3%, which is bigger than most functionalized-MSN studies (less than 10%), while DLC for DOX@MSN was much higher (around 23.8 ± 0.2%). This could be attributed to the fact that MSN without anchored extended polymer chains could have less hindrance to encapsulate guest molecules like DOX here in this study. The more extended polymer chains could decrease the loaded drug consistently in the polymeric silica particles.

The results showed that, the release of DOX@MSN (with-

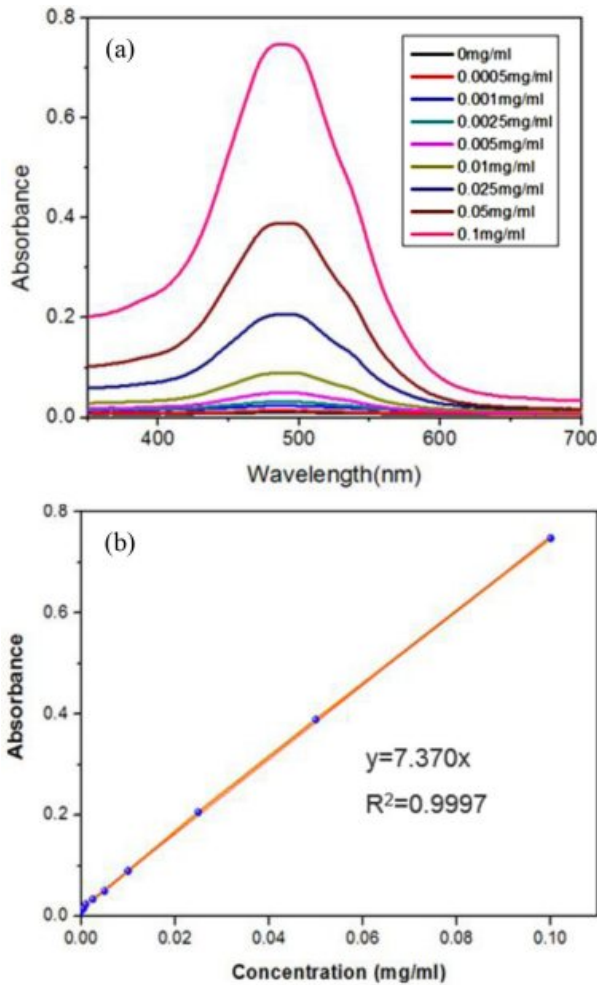


**Figure 5.** UV-vis absorption spectra of DOX in Milli-Q water at different concentrations (a); the resultant calibration curve based on plotting the absorbance at 480 nm against the concentration of DOX (b).

out polymers) at three different pH values was somewhat pH dependent, because of the presence of silanol groups on the external surface of MSN that can be affected with pH changes as indicated in Figure 6. However, the release process related to this system was still very small without good control and no clear difference between the three pH values (although it was a little bit higher in acidic medium than the neutral one).

On the other hand, the anchored copolymer can act as a smart cap for the acid-triggered release of DOX from silica pores at the same pH values and consequently provide a more clearly pH-dependent system. As illustrated in Figure 7, only 14% of conjugated DOX was released from the DOX@hybrid after incubation for one day at pH 7.5, suggesting that lots of DOX molecules were still covalently conjugated within the

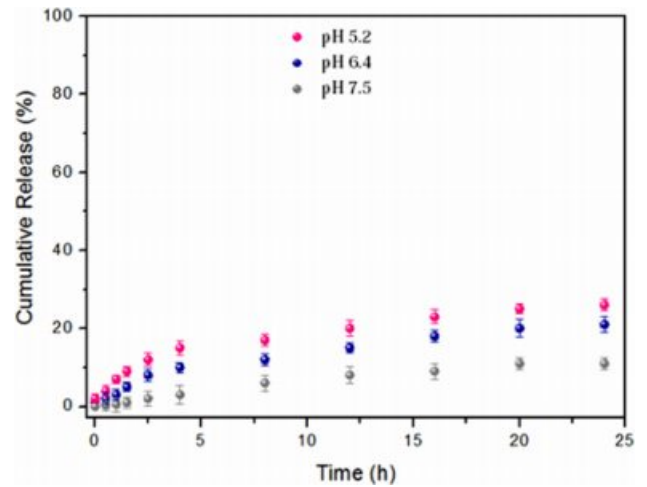


**Figure 6.** *In vitro* pH-dependent release profiles for DOX@MSN under three different pH conditions.

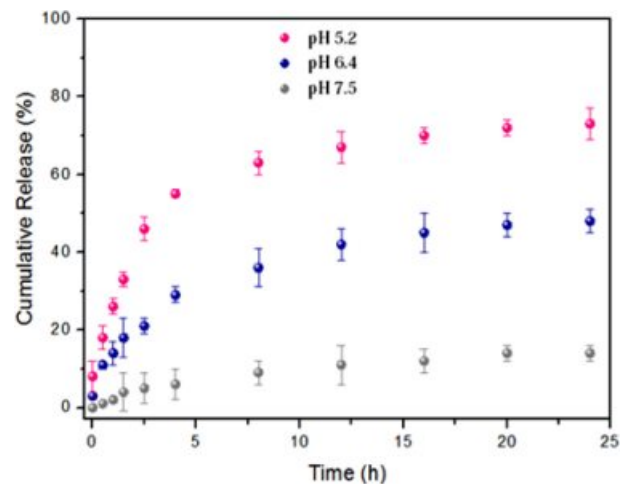


**Figure 7.** *In vitro* pH-dependent release profiles of DOX@hybrid at three different pH conditions.

nanocontainers. By contrast, the released amount of DOX dramatically reached 48% and 73% at pH 6.4 and 5.2 during the same number of hours, respectively. Therefore, such pH response for these polymeric nanomaterials can trigger the programmed release of encapsulated payloads in a successful way, especially in weak acidic environment, which is a key role for intracellular antitumor efficacy.

## Conclusions

In this study, pH-responsive mesoporous silica nanoparticles based on MPS and DMAEMA monomers were successfully prepared via a simple one-step reaction. A series of char-

acterization methods were applied to confirm the structures of obtained nanoparticles. The results showed that, the anchored copolymers can act as smart caps for the on-off triggered release of DOX at three different pH values. Moreover, the *in vitro* drug release tests have been investigated at two different techniques with the presence and the absence of the grafted copolymers, leading to a clear difference in the released drug profiles. Overall, such reverse pH release behavior can be helpful in designing potent biopolymeric materials when a continuous release of a drug is desired at low pH values e.g. various tumors and inflammations.

**Acknowledgments:** The authors thank NSFC (grant number 21871069) and Open Project of Key Laboratory of Microsystems and Microstructures Manufacturing (2016KM003) for financial supports.

## References

1. J.-Y. Shin, D. Y. Lee, Y.-S. Song, and B.-Y. Kim, *Polym. Korea*, **42**, 967 (2018).
2. N. Rahoui, P. Zhou, N. Taloub, M. Hegazy, and Y. D. Huang, *IOP Conf. Series: Mat. Sci. Eng.*, **389**, 012009 (2018).
3. N. Rahoui, M. Hegazy, B. Jiang, N. Taloub, and Y. D. Huang, *Am. J. Anal. Chem.*, **9**, 273 (2018).
4. Y. Kim, S. Lee, D. Kim, K. Noh, K. S. Oh, S. Cho, E. Choi, K.-p. Kim, and K. M. Huh, *Polym. Korea*, **42**, 1059 (2018).
5. P. Zhou, L. Wang, G. Wu, Y. Zhou, M. Hegazy, and X. Huang, *ChemistrySelect*, **2**, 6249 (2017).
6. G. Wu, X. Liu, P. Zhou, L. Wang, M. Hegazy, X. Huang, and Y. Huang, *Mater. Sci. Eng. C*, **94**, 524 (2019).
7. M. Lim, J. Park, J. Song, and H.-I. Kim, *Polym. Korea*, **42**, 1091 (2018).
8. D. Su, X. Liu, L. Liu, L. Wang, H. Xie, H. Zhang, X. Meng, and X. Huang, *Adv. Funct. Mater.*, **28**, 1705699 (2018).
9. L. Wang, Y. Lin, Y. Zhou, H. Xie, J. Song, M. Li, Y. Huang, X. Huang, and S. Mann, *Angew. Chem. Int. Ed.*, **58**, 1067 (2019).
10. B.-R. Kim, S. K. Jeoung, Y. K. Ko, J. U. Ha, Y. W. Kim, S. Y. Lee, J. Kim, J. H. Lee, and P.-C. Lee, *Polym. Korea*, **42**, 1030 (2018).
11. D. Su, J. Qi, X. Liu, L. Wang, H. Zhang, H. Xie, and X. Huang, *Angew. Chem. Int. Ed.*, **58**, 3992 (2019).
12. M. Hegazy, P. Zhou, G. Wu, L. Wang, N. Rahoui, N. Taloub, X. Huang, and Y. Huang, *Polym. Chem.*, **8**, 5852 (2017).
13. N. Rahoui, B. Jiang, M. Hegazy, N. Taloub, Y. Wang, M. Yu, and Y. D. Huang, *Colloids Surf. B: Biointerf.*, **171**, 176 (2018).
14. A. Mehmood, H. Ghafar, S. Yaqoob, U. Gohar, and B. Ahmad, *J. Dev. Drugs*, **6**, 1000174 (2017).
15. Y. Wang and H. Gu, *Adv. Mater.*, **27**, 576 (2015).
16. X. Huang, N. Hauptmann, D. Appelhans, P. Formanek, S. Frank, S. Kaskel, A. Temme, and B. Voit, *Small*, **8**, 3579 (2012).
17. D. Yadav, S. Suri, A. Chaudhary, M. Beg, V. Garg, M. Asif, and A. Ahmad, *Polish J. Chem. Tech.*, **14**, 57 (2012).
18. Y. Yan, A. P. Johnston, S. J. Dodds, M. M. Kamphuis, C. Ferguson, R. G. Parton, E. C. Nice, J. K. Heath, and F. Caruso, *ACS Nano*, **4**, 2928 (2010).
19. Y. Liu, M. Li, F. Yang, and N. Gu, *Sci. China Mater.*, **60**, 471 (2017).
20. S. Mura, J. Nicolas, and P. Couvreur, *Nat. Mater.*, **12**, 991 (2013).
21. C.-Y. Hong, X. Li, and C.-Y. Pan, *J. Mater. Chem.*, **19**, 5155 (2009).
22. Y. Zhang, C. Y. Ang, M. Li, S. Y. Tan, Q. Qu, Z. Luo, and Y. Zhao, *ACS Appl. Mater. Interfaces*, **7**, 18179 (2015).
23. N. Orakdogan, *Polym. Eng. Sci.*, **53**, 734 (2013).
24. I. Mileto, E. Bottinelli, G. Caputo, S. Coluccia, and E. Gianotti, *Phys. Chem. Chem. Phys.*, **14**, 10015 (2012).
25. S. El-Hamouly, M. Azab, A. S. M. Diab, and M. Hegazy, *Asian J. Chem.*, **24**, 176 (2012).
26. M. Hegazy, S. El-Hamouly, M. Azab, S. Beshir, and M. Zayed, *Polym. Sci. Series B*, **56**, 182 (2014).
27. N. Rahoui, B. Jiang, N. Taloub, M. Hegazy, and Y. D. Huang, *J. Biomater. Sci., Polym. Ed.*, **29**, 1 (2018).
28. F. Jafari-soghieh and H. Behniafar, *Polym. Korea*, **43**, 52 (2019).
29. N. Taloub, L. Liu, N. Rahoui, M. Hegazy, and Y. Huang, *Polym. Test.*, **75**, 344 (2019).
30. B. Choi and J. S. Kim, *Polym. Korea*, **43**, 156 (2019).
31. G. Wu, X. Liu, P. Zhou, Z. Xu, M. Hegazy, X. Huang, and Y. Huang, *Mater. Sci. Eng. C*, **99**, 1153 (2019).
32. P. Zhou, S. Wu, X. Liu, M. Hegazy, G. Wu, and X. Huang, *ACS Appl. Mater. Interfaces*, **10**, 38565 (2018).
33. N. Taloub, A. Henniche, L. Liu, J. Li, N. Rahoui, M. Hegazy, and Y. Huang, *Comp. Part B: Eng.*, **163**, 260 (2019).